Annals of Biomedical Engineering (© 2022)
https://doi.org/10.1007/s10439-022-03006-y

BMES BIOMEDICAL ENGINEERING SOCIETY

Original Article

Proper Orthogonal Decomposition Analysis Reveals Cell Migration Directionality During Wound Healing

SUYUE HAN,[1] DUY T. NGUYEN,[1] YAHYA MODARRES-SADEGHI,[1] and JUAN MIGUEL JIMÉNEZ[1,2]

[1]Department of Mechanical & Industrial Engineering, University of Massachusetts Amherst, Amherst, MA 01003, USA; and [2]Department of Biomedical Engineering, University of Massachusetts Amherst, Amherst, MA 01003, USA

(*Received 31 December 2021; accepted 1 July 2022*)

Associate Editor Stefan M. Duma oversaw the review of this article.

Abstract—A proper orthogonal decomposition (POD) order reduction method was implemented to reduce the full high dimensional dynamical system associated with a wound healing cell migration assay to a low-dimensional approximation that identified the prevailing cell trajectories. The POD analysis generated POD modes that were representative of the prevalent cell trajectories. The shapes of the POD modes depended on the location of the cells with respect to the wound and exposure to disturbed (DF) or undisturbed (UF) fluid flow where the net flow was in the antegrade direction with a retrograde component or fully antegrade, respectively. For DF and UF, the POD modes of the downstream cells identified trajectories that moved upstream against the flow, while upstream POD modes exhibited sideways cell migrations. In the absence of flow, no major shape differences were observed in the POD modes on either side of the wound. The POD modes also served to reconstruct the cell migration of individual cells. With as few as three modes, the predominant cell migration trajectories were reconstructed, while the level of accuracy increased with the inclusion of more POD modes. The POD order reduction method successfully identified the predominant cell migratory trajectories under static and varying pulsatile fluid flow conditions serving as a first step in the development of artificial intelligence models of cell migration in disease and development.

Keywords—Cell migration, Endothelialization, Wound healing, Proper orthogonal decomposition, POD, Shear Stress, Endothelial.

Address correspondence to Juan Miguel Jiménez, Department of Biomedical Engineering, University of Massachusetts Amherst, Amherst, MA 01003, USA. Electronic mail: juanjimenez@umass.edu

INTRODUCTION

Cell migration in wound healing is a highly complex process that is not only regulated by the extracellular matrix composition, and paracrine and autocrine signaling, but also by local mechanical forces that are converted into biochemical signals.[8,10,14,31] Mechanical forces due to fluid flow are a major determinant of cell phenotype in blood and lymphatic vessels, especially in development and disease, and have been shown to influence cell migration both *in vitro* and *in vivo*.[1,8,12,14,16,32,33] Developing models that can describe cell migration under different mechanical forces is critical for understanding the role of fluid flow on wound healing. Some mathematical models of cell migration have primarily focused on highly simplified cases describing the displacement of few individual cells or the edge of a cell monolayer using scratch-wound-like assays.[9,21] Fisher's population growth and wave propagation equation have been used to model the displacement of the cell wound edge.[11,21] However, this method treated the wound edge as a constant-speed traveling wave and failed to capture the cell wound edge transient accelerating and decelerating phases,[13] which are characteristics of cell migration when cells are exposed to fluid flow.[14] The migration of individual cells in homogeneous environments can be described using modified random walk models,[6] however introduction of the interaction with neighboring cells and external stimuli, such as fluid flow, makes modeling the migration of many cells very challenging without additional biological data. Some single cell migration dynamics models are insufficient to describe the migration of large numbers of cells,[19] while other

Published online: 11 July 2022

detailed single cell models become computationally expensive when expanded to larger cell populations.[2,5,7,24] Although many different models, such as phase-field, polygonal, cellular Potts, and spherical cells have elucidated biological mechanisms of cell migration, few cell migration models exist that consider molecular mechanisms of individual cells and relate it to the tissue dynamics and collective cell migration given that the assumptions at one level affect the next level and the complexity of the models make the operational realm difficult to define.[4] Model efficacy can strongly depend on the distribution of cells. Cell migration where varying levels of cell confluency exist after a multifocal injury are better suited for cellular Potts and center-based models, while inappropriate for vertex based models where neighboring cells share edges and nodes and these would need to be replicated to properly model breakaway cells.

To address some of the challenges described above, proper orthogonal decomposition (POD) was implemented to characterize and reconstruct cell displacements in a wound healing assay, where levels of cell confluence varied temporally, under different fluid flow conditions. POD is not a mathematical model that can consider the biochemical reactions and biophysical interactions of a migrating cell. Instead, POD is a principal component analysis technique that enables analysis of complex multi-dimensional data sets and provides optimal-ordered, orthogonal bases to represent the data in a least-square sense.[25,27,28] Cell migration trajectories are characterized by sudden changes in direction and persistent displacements, which can be spectrally represented by a range of frequencies. This attribute of cell migration is exploited to decompose the different cell motions into a set of deterministic functions that describe cell migration of large numbers of cells using simpler functions.

MATERIALS AND METHODS

POD analyses were conducted on previously published cell migration data that focused on the effects of fluid flow characteristics on cell migration.[22] A thorough analysis of cell velocity, mean square displacement, and other important parameters are thoroughly covered in[22] along with an extensive description of the experiments.

Cell Culture

Human umbilical vein endothelial cells (passage 3–10; Lonza, Basel, Switzerland) were kept at 37 °C in 5% CO_2 humidified air. HUVECs were grown in EGM-2 cell medium supplemented with 2% FBS (Lonza, Basel, Switzerland).

Wound Healing Experiments

HUVECs were seeded on 0.1 mg/mL fibronectin (BD Biosciences, Bedford, MA) coated PDMS (Sylgard 184, Dow, Midland, MI) membranes. Forty-eight hours after reaching 100% confluence, the PDMS block was removed and the HUVECs were incubated in Hoechst 33342 (Fisher Scientific, Pittsburgh, PA) at a 1.0 μg/mL concentration in EGM-2 serum-free cell medium for 30 min at 37°C, 5% CO_2 humidified air (Fig. 1a). After washing with phosphate-buffered saline solution (PBS) at 37°C, 25mM HEPES buffer concentration EGM-2 cell medium was added and the cells were placed in either a Petri dish for the static condition or a parallel plate flow chamber (PPFC) for the pulsatile flow conditions as previously described.[17,22] The test section of the PPFC where the cells were located had a height of 1 mm and a width of 57 mm yielding an aspect ratio of 1:57 to promote a uniform flow field away from the side walls where the cells were located. Cells were exposed to either static conditions or one of two pulsatile waveforms generated with a 520U Watson Marlow peristaltic pump (Cornwall, UK) and a data acquisition card (USB-6229, National Instruments) (Fig. 1b). The pulsatile flow rate was varied temporally by varying the angular velocity of the pump head. The fluid flow rate was measured (Transonic Systems, Inc., Ithaca, NY, USA) at the inlet of the PPFC and the wall shear stress (WSS) was approximated to range between −0.11 Pa and 0.19 Pa with a mean of 0.04 Pa for disturbed flow (DF), while ranging between 0.23 and 0.54 Pa with a mean of 0.39 Pa for undisturbed flow (UF) (Fig. 1b). The waveforms were classified as undisturbed or disturbed if the oscillatory shear index (OSI) was zero or nonzero, respectively. The oscillatory shear index was determined as follows

$$\mathrm{OSI} = \frac{1}{2}\left(1 - \frac{\left|\int_0^T \mathrm{WSS}\ dt\right|}{\int_0^T |\mathrm{WSS}|\ dt}\right), \tag{1}$$

where T is the period of integration and WSS is the tangential stress experienced by the endothelial cells. OSI equals 0 when the fluid flow is moving in the antegrade direction throughout the period, while a nonzero OSI value corresponds to the condition where flow reverses for a portion of the time period T. Epifluorescence microscopy images were captured every 30 min up to 60 h. The experiments were conducted inside a constant temperature environmental chamber at 37°C (In Vivo Scientific, St Louis, MO). The initial

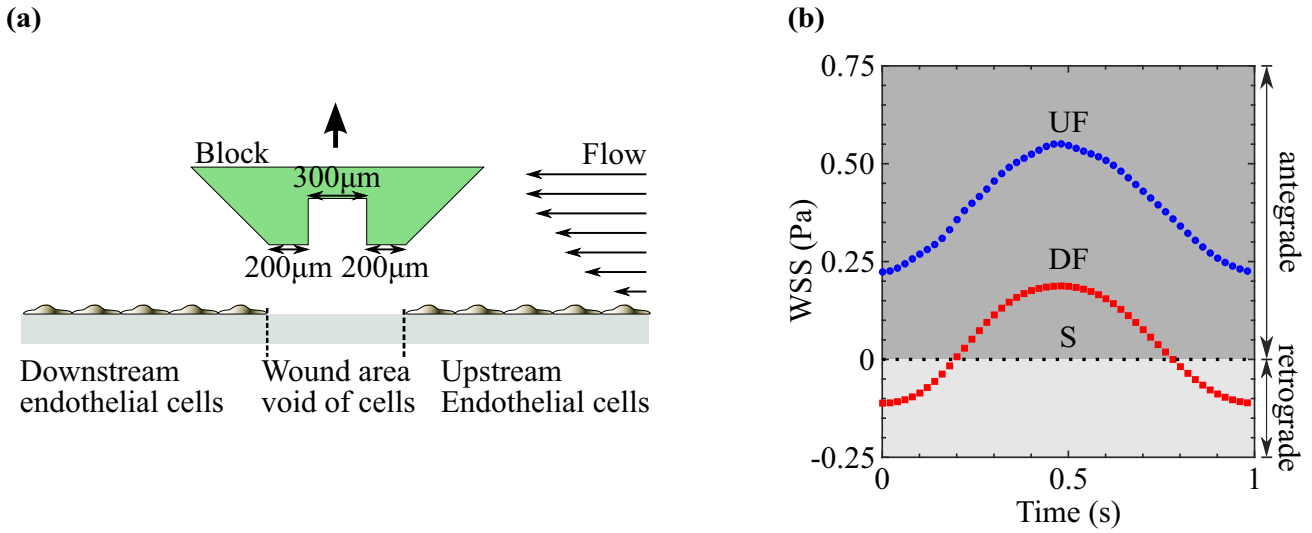

FIGURE 1. (a) A block generated a gap between upstream and downstream HUVECs. The cells were classified as upstream or downstream with regard to their location at the start of the experiment. The PDMS block is not drawn to scale. Flow is from right to left. (b) Once the block was removed, HUVECs were exposed to static (S), disturbed flow (DF), or undisturbed flow (UF) conditions with varying levels of wall shear stress (WSS) values for every period during a wound healing assay.

cell tracking was conducted using Imaris software and edited manually with ImageJ software.

Proper Orthogonal Decomposition Analysis of Cell Migration

The proper orthogonal decomposition method was used to obtain the dominant mode set related to endothelial cell displacement.[25,27,28] POD methods reduce the dimensions of a system by projecting the original system onto a subspace consisting of a set of bases, called POD modes, such that the first few modes contain most of the energy of the original system.

An ensemble of snapshots, $u_i(t) = u(c_i, t)$, is selected from the cell velocity data $u(\mathbf{c}, t)$, where c_i refers to the cell i, and $i = 1, ..., M$, where M is the total number of cells. A set of proper orthogonal bases are defined as $\Phi = \{\phi_i(t) | i = 1, ..., m\}$, such that it minimizes the least square distance, $\| \mathbf{u} - \Pi\mathbf{u} \|$, between the snapshots $\mathbf{u} = \{u_i(t)\}_{i=1}^{M}$ and its reduced order solution, where $\Pi = \sum_{i=1}^{m} \phi_i \phi_i^T$ is the orthogonal projection. This minimization problem, Q, is represented as

$$Q = \min_{\Phi \in L^2(C)} \| \mathbf{u} - \Pi\mathbf{u} \|^2 . \tag{2}$$

Mathematically, the solution of Φ is equivalent to the solution of the optimization problem H where

$$H = \max_{\Phi \in L^2(C)} \frac{\langle (\mathbf{u}, \Phi)^2 \rangle}{\| \Phi \|^2}, \tag{3}$$

and (., .) and ||.|| denote the L^2 inner product and L^2 norm over the cell space, C, while $< . >$ denotes a statistical average operator. In these equations, Q and H simply represent the minimization and maximization problems that need to be solved to find the proper orthogonal bases, Φ, for an optimal representation of the cell velocity field, u.

If the snapshots are adequate to describe the system, the above problem can be addressed by solving the eigenvalue problem

$$\mathbf{C}A_i = \lambda_i A_i, \tag{4}$$

where A_i are the system's eigenvectors with eigenvalues of λ_i, and eigenvectors of $\mathbf{C}$, which can be found as $\mathbf{C} = \mathbf{u}\mathbf{u}^{\mathbf{T}}$. These eigenvectors are then called the POD modes.

Instead of generating spatial modes, as is customary, temporal modes are generated to analyze the displacement of individual cells. By generating the temporal modes, the velocity time series for each cell is considered as one snapshot, so that the POD subspace contains the temporal information, and a combination of these temporal modes represents the displacements of the cells over time. By doing so, one point in the POD temporal subspace represents the velocity of one cell as it changes over time. Once the dominant modes of the cell velocity are determined, the trajectory modes can be constructed by integrating the velocity modes over time. Because the first few POD modes contain most of the kinetic energy of the original system, the first few velocity or trajectory modes represent the most energetic patterns of the cell motions.

Data Processing and POD

An in-house Matlab program was written for data processing and implementation of the POD analysis on the cell migration data set. Several machine learning and computer geometry concepts were implemented. First, the raw data were processed for removal of discontinuities and nonuniformities from the data set. Signal continuity was examined by building a matrix containing all the tracking information for all data points. The data points properly tracked were marked as 1 and the points not properly tracked as 0, and the points that were not tracked continuously were removed. The data were re-sampled to smooth out any nonuniformities in the tracking time steps. Then, the machine learning technique called clustering was used to identify cells as belonging to either downstream or upstream cell groups. After identification of the cell clusters, an edge finder technique was used to determine the wound edge for each time step. In this step, a bounding box was generated for the cell cluster identified in the previous step, and the front edge of the wound was defined as the inner edge of two neighboring bounding boxes. To find the leading-edge, another computer geometry concept called meshing was used to calculate the distance from the cell to the actual wound edge. Then, at every time step the locations of the cells on the wound edge were used as the base nodes for generating a new 2D hexahedral mesh. Every cell occupies a hexahedral element and allows for calculation of the distance between each cell and the wound edge.

Once the cells were grouped into upstream or downstream clusters, POD velocity modes were generated independently for each cluster. These velocity modes were integrated to yield the displacement modes. After determining the trajectory modes, the cells were further grouped based on their distance from the wound edge and the mode values of these cell subgroups were calculated. The contribution of modes for different cell groups was obtained by organizing a collection of mode amplitude distributions into histograms.

RESULTS

Wound Healing

Wound healing experiments were conducted to assess the role of pulsatile fluid flow with and without flow reversal in cell migration (Fig. 1b). A polydimethylsiloxane (PDMS) membrane was coated with fibronectin overnight before seeding with human umbilical vein endothelial cells (HUVECs). Traditional scratch wound assays where cells, and consequently underlying extracellular matrix (ECM) proteins, are removed when the monolayer reaches confluence can potentially affect cell migration direction and velocity due to ECM protein concentration gradients caused by the mechanical scratch. To avoid the introduction of ECM protein concentration gradients, a PDMS block was used to restrict the growth of endothelial cells and upon removal of the PDMS block, response to wound healing could be assessed successfully (Fig. 1a).[23,26] Forty-eight hours after reaching confluence, the PDMS block was removed and the cell-coated PDMS membranes were placed in a Petri dish under static (ST) conditions or in a parallel plate flow chamber (PPFC) exposed to pulsatile disturbed (DF) or undisturbed (UF) flow to recreate fluid flow characteristics present in arterial sites that are susceptible or resistant to atherosclerosis, respectively.[35] HUVECs migrated in the direction of the wound at varying rates depending on the side of the wound and the flow conditions. The cell displacements were tracked for up to 60 h. Then, the tracks for the upstream and downstream HUVECs were decomposed using proper orthogonal decomposition (POD).

Proper Orthogonal Decomposition of Cell Trajectories

The cell displacements and time delay between each image yielded a velocity value for each cell that served as an input for the POD analysis to generate the POD velocity modes. The POD trajectory modes were then generated by integration of the velocity modes. Once the POD modes are determined, the total trajectory of all cells, D, can be written as

$$D = \sum_{i=1}^{N} a_i \psi_i, \tag{5}$$

in which ψ_i are the POD trajectory modes, a_i are the coefficients with the corresponding mode amplitude, and N is the total number of POD modes used in constructing the cell trajectory. The contribution of each mode in the total trajectory of a cell is proportional to the amplitude of the coefficient a_i. The length of the POD trajectory modes, ϕ_i, is dimensionless, while the coefficient a_i has the unit of length.

As is customary for POD modes, the modes are organized in a descending order with mode 1 being the most energetic mode as shown in Fig. 2a for the downstream HUVECs of the DF condition. The first six modes accounted for 51.3, 7.3, 6.2, 4.9, 4.1, and 3.5% of the energy content, respectively. Summing the energy content due to these first six modes equals 77.4%. By organizing the modes in descending order, the dominant migratory trajectories can be identified. Figure 2b shows the first 6 dominant POD trajectory

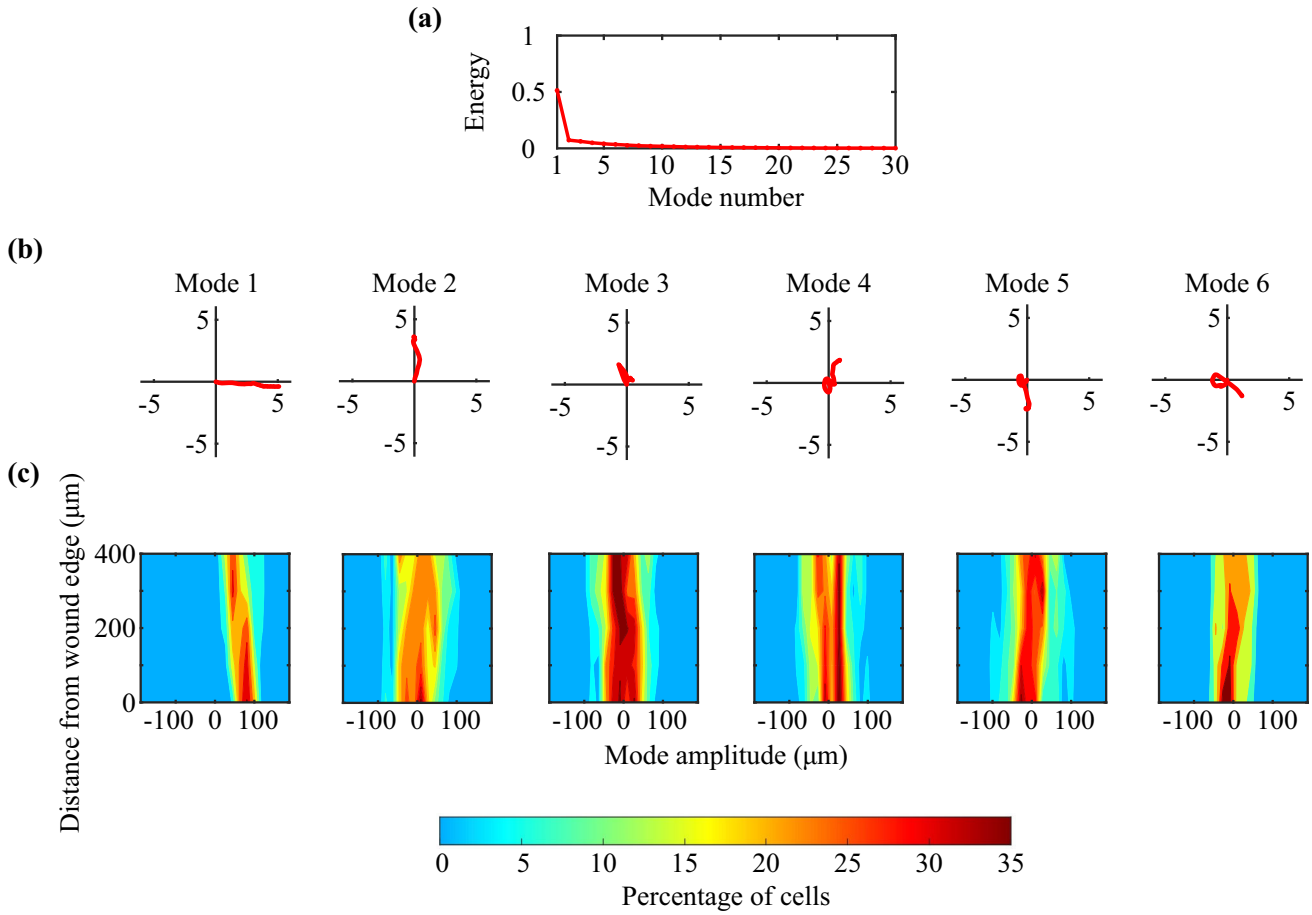

FIGURE 2. HUVECs trajectories in a wound healing assay under pulsatile DF on the downstream side of the wound were analyzed using proper orthogonal decomposition. (a) The kinetic energy distribution decreases rapidly for the 30 most energetic modes. The POD modes highlight the six most energetic (b) cell trajectory shapes and (c) the histogram of the corresponding mode amplitude coefficients with respect to the distance from the leading edge of the wound. The product of the POD mode shape and mode amplitude coefficients defines the trajectory and contribution of a particular population of cells within the wound. In (b) an abscissa and ordinate correspond to a normalized horizontal and vertical displacement, respectively.

modes for the downstream HUVECs of the DF condition. The dominant trajectory mode, mode 1, displays persistent migratory trajectories of HUVECs against the flow from left to right or downstream to upstream per the experimental coordinates. The second most energetic mode, mode 2, represents a trajectory of HUVECs moving directly sideways perpendicular to the bulk fluid flow direction. Modes 3 to 6 represent more complicated cell displacement paths where HUVECs move in one direction and then turn to another direction along with circular-type displacements.

To assess the effect of distance from the wound edge, the viewing window was divided into a series of 100 μm wide by 2.25 mm long sub-regions, starting and moving away from each wound edge in 100 μm increments. Figure 2c shows histograms of the percentage of cells that have coefficients a_i with a mode amplitude between − 189 μm and + 189 μm. The mode amplitude histograms are determined by projecting the original cell migration displacements onto the POD modes. Each cell contributes to the histogram and different cells can have different mode amplitude values for each corresponding mode. A larger mode amplitude corresponds to a greater contribution of that mode toward the total cell displacement.

The POD modes can play an important role in assessing if a wound is closing or opening by considering both the shape of the POD trajectory mode and the sign of the mode amplitude. For this reason, the POD trajectory mode shapes in Fig. 2b are plotted such that a positive mode amplitude in Fig. 2c represents a cell displacement toward the wound and a negative mode amplitude corresponds to a cell displacement away from the wound.

For mode 1, the vast majority of cells within 0 and 100 μm from the edge of the wound display a nonzero mode amplitude, which decreases as the distance

increases away from the wound edge, highlighting the spatial dependence of this mode (Fig. 2c). For modes 2 to 6, the magnitudes of the mode amplitude coefficients are close to zero for the majority of the cells, emphasizing the minimum influence of these modes on the cell trajectories.

Figure 3a shows the first three dominant trajectory modes for the upstream and downstream cells for the ST, DF, and UF conditions. The modes are sorted in a manner where the first mode captures most of the energy. When exposed to static conditions, the most energetic trajectory modes on the downstream and upstream sides represent cell displacements predominantly in the direction of closing the wound with smaller superposed motions, as shown by the positive values of the mode amplitude coefficients in Fig. 3b. Exposure of HUVECs to DF, where the flow reverses for a short interval, causes greater changes in the motion of the upstream cells. On the downstream side, the most energetic trajectory mode, mode 1, is directed upstream, while the second and third modes indicate spanwise and turning cell movements. In contrast, the trajectory modes 1 to 3 for the HUVECs on the upstream side of the wound indicate primarily sideways movements, highlighting that the closure of the wound is predominantly completed by the downstream cells migrating against the flow. A similar observation is made for the UF case where the flow is also pulsatile, while fully antegrade. The trajectory of the downstream cells, as indicated by the three most energetic modes, is described by an upstream migration that is closing the wound, although less direct than the DF trajectory mode 1, with turns and reversals in the migration direction. In contrast to downstream modes 1 to 3, the most energetic modes for the upstream HUVECs suggest a predominant sideways migration that plays a less important role in closing the wound.

The mode amplitude histograms of Fig. 3b show the distribution of the mode amplitude coefficients a_i for the ST, DF, and UF conditions. For the static case, the mode amplitudes for modes 1, 2, and 3 are scattered between -189 and 189 μm with a larger number of cells displaying positive mode amplitudes suggestive of a closing wound. When HUVECs are exposed to DF, the mode 1 amplitude histogram for downstream HUVECs assumes a narrower distribution with about 35.2% of the cells represented by a mode amplitude of 81 μm near the wound edge. As the distance increases away from the wound edge, the histogram peak goes toward zero, suggesting that the trajectory represented

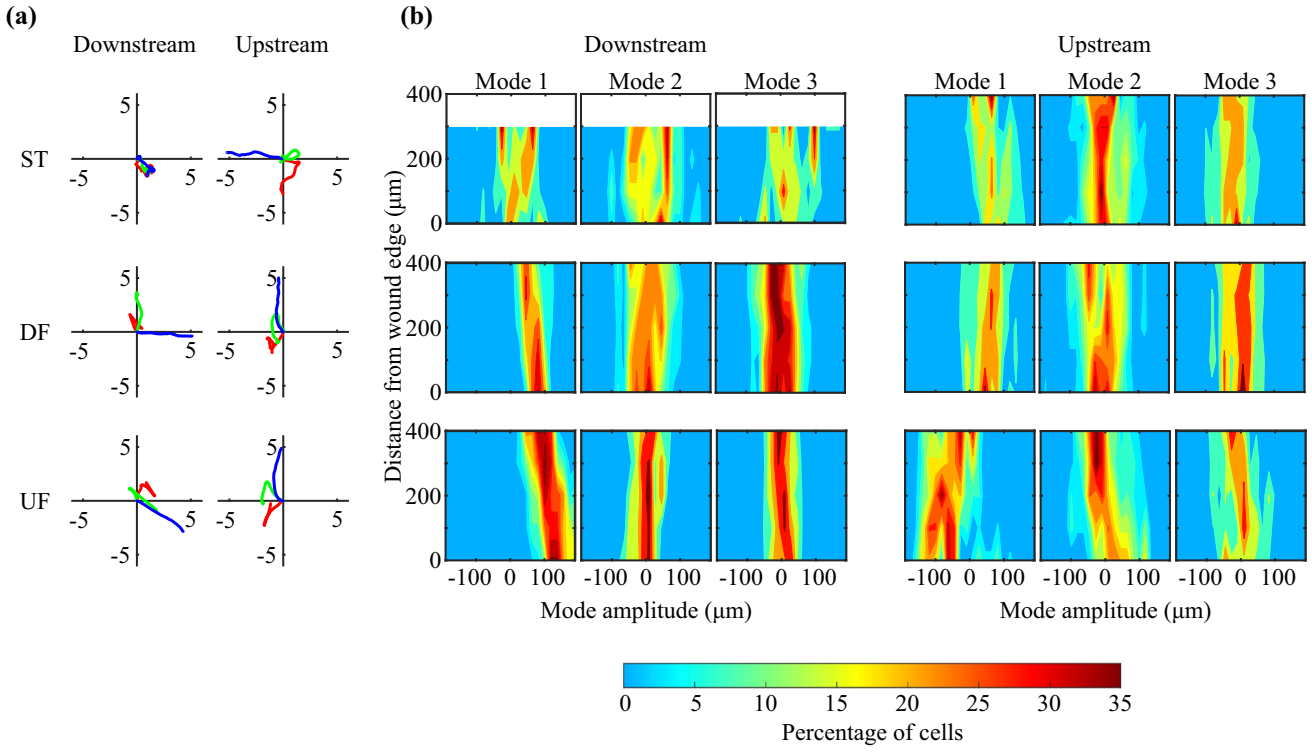

FIGURE 3. (a) POD trajectory modes and (b) histograms of the corresponding mode amplitude coefficients as a function of distance away from the wound for the downstream and upstream cells in a wound healing assay exposed to ST, DF, and UF. The POD modes are generated using the trajectories of upstream or downstream cell clusters and sorted in an energy-intensity descending order. The three most energetic trajectory modes: mode 1 (blue), mode 2 (green), and mode 3 (red) are displayed with dimensionless axes. An abscissa and ordinate correspond to a normalized horizontal and vertical displacement, respectively. The histograms show the mode amplitude coefficient distributions for all cells as a function of distance away from the wound edge.

by mode 1 is more dominant for cells near the edge than for those farther away from the edge. The mode 1 amplitude histogram for the upstream cells displays a broader distribution with a peak around 45 μm near the wound edge that decreases in cell percentage as the distance increases from the edge. Mode amplitude histograms for modes 2 and 3 on the downstream and upstream sides for the DF case are broader and centered about a mode amplitude of approximately 0 μm, suggesting a smaller contribution by these modes. The mode 1 amplitude distribution for the downstream cells exposed to UF shows the greatest percentage of cells at around 117 μm near the wound edge and the percentage decreases as the distance increases from the wound edge, while the peak amplitude remains relatively high at about 81 μm. Mode amplitude distributions for modes 2 and 3 for the downstream HUVECs are relatively similar, with histogram distributions closely centered about 0 μm, which suggests a minimal influence by trajectory modes 2 and 3 on the downstream cells. The shape of POD trajectory mode 1 for the upstream HUVECs exposed to UF suggests that the cells are initially moving toward closing the wound and then turning. However, the product of the POD trajectory mode and the mode amplitude coefficient for each cell per Eq. (5) shows that the upstream HUVECs are initially moving upstream against the flow and further increasing the size of the wound and eventually turning to close the wound. It is important to note that the majority of the mode 1 amplitude coefficients for upstream HUVECs exposed to UF have a negative sign and when multiplied by POD trajectory mode 1, a right moving trajectory becomes a left moving trajectory, while an up moving trajectory becomes a down moving trajectory. For modes 2 and 3 of the upstream cells exposed to UF, the mode amplitude peaks at the edge of the wound shift toward -27 μm as the distance from the edge of the wound increases, emphasizing how cells close and away from the wound edge react differently to UF conditions. The mode amplitude coefficient in combination with the POD trajectory mode shape data clearly demonstrate that the cell migration and trajectory are influenced by both the flow condition and the distance from the wound edge.

One of the advantages of the POD analysis for cell migration characterization is the capacity of reconstructing the trajectories with a fraction of the original information (Fig. 4). The POD-reconstructed cell migration trajectories can be calculated using Eq. (5). The original data set encompassed up to 60 h of cell tracking every 30 min for thousands of cells. Being able to extract the information of interest here, which is to identify the predominant cell trajectories that contribute to wound healing without the superposed random-like displacements that can characterize cell movements, minimizes the amount of data to post-process and can aid in the reconstructions of the cell trajectories. Figure 4 shows the reconstruction of the cell migration for the ST, DF, and UF conditions. For the DF and UF cases, information from only 3 modes shows the migration of downstream cells against the flow to close the wound, and the migration of upstream cells in a direction perpendicular to the flow. For the ST case, the upstream and downstream migration is more homogeneous although less evident given that less cells are present on the downstream side. The number of modes is increased from 3 to 6 to 12 to 24 and for the DF and UF cases the contribution of the downstream cells in closing the wound is evident, while a smaller contribution from the upstream cells is also observed. For the ST case, although both sides contribute to closing the wound, the apparent dominance of upstream cells is due to the larger number of cells on the upstream side. When the number of modes is increased to 192 for the ST, DF and UF cases, more complicated cell paths become evident due to the addition of lower-energy modes. Two identical endothelial cell (EC) displacement paths emerge when data from 192 modes are compared with the original data set.

DISCUSSION

The directionality of cell migration is a fundamental response to tissue injury and can be affected by the type of injury, chemoattractant gradients, interruption of the contact inhibition homeostasis, sudden opening in tissue due to cell removal, cell proliferation, mechanical signals, endogenous electrical fields, and fluid flow.[3,36] For endothelial cells, which are exposed to fluid flow, the migration rate and directionality are dependent on the characteristics of the flow field.[3] Although challenging, modelling the individual displacement of large numbers of cells can be instrumental in understanding the healing process of an injury that is exposed to fluid flow. In contrast to modeling, here we use experimental cell migration data to show that the complex migratory response of thousands of cells to different fluid flow waveforms can be represented as a summation of a series of POD modes, and important information about the directionality of cell migrations can be extracted from only a few of these POD modes.

The key finding of this study is that the individual trajectories of large numbers of cells can be recreated using the POD order reduction method to reduce the full high-dimensional dynamical system to a low dimensional approximation. The results showed that inclusion of only a few of the most energetic modes can

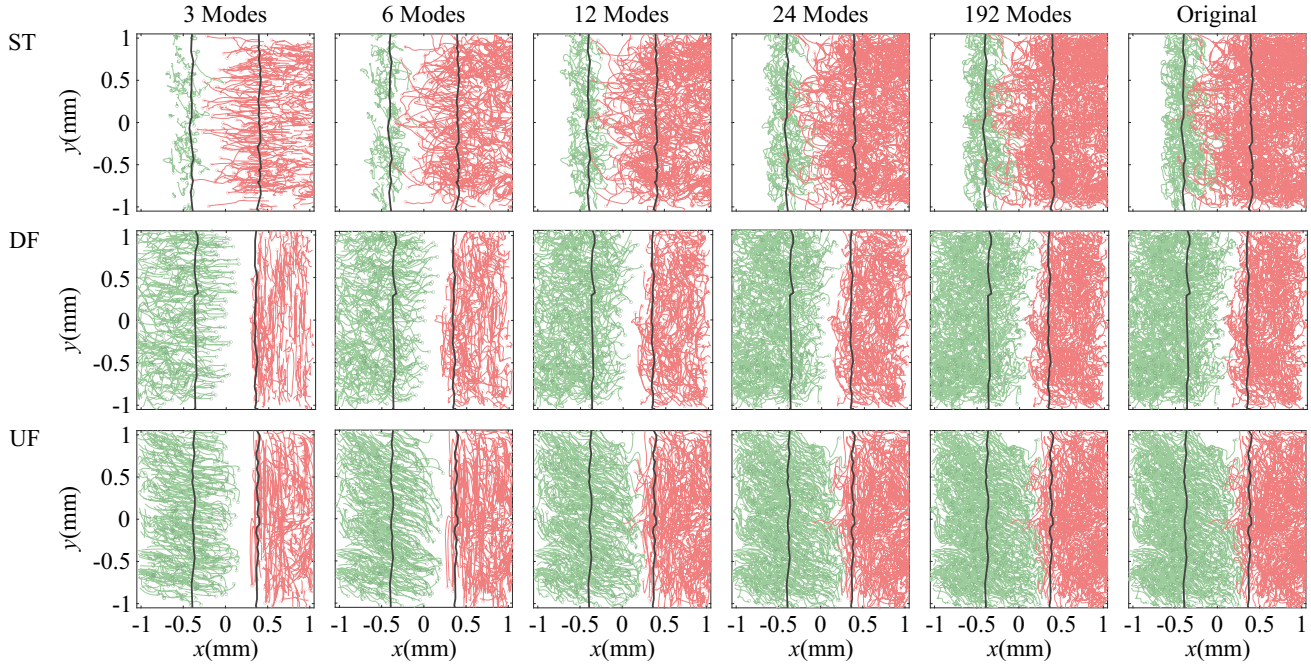

FIGURE 4. Comparison of cell trajectories reconstructed using 3, 6, 12, 24, and 192 POD modes versus the original cell trajectories for the three different experimental conditions: ST, DF, and UF. The wound edge at time equal zero is plotted in black.

recreate the cell trajectories. The less common trajectories were absent from the most energetic modes, and the reconstructed trajectories accurately recreated the predominant cell movements (Fig. 4). In comparison with traveling wave, continuum cell population, and leading edge tracking models where the invading cell front is modelled without details of the individual cell displacements near and far from the cell front,[18,20,21,29,34] the POD order reduction analysis included the predominant cell movements for all cells throughout the monolayer. The most energetic mode for the downstream side represented cells predominantly migrating upstream regardless of the presence or absence of flow, while the most energetic mode for the upstream side exhibited similar trends only under static conditions where upstream cells move primarily downstream to close the wound. These results highlight the importance of understanding how the presence of fluid flow can affect wound healing in a blood vessel after vascular intervention. Wound healing, as defined by reendothelialization of an artery after vascular intervention, is one of the primary clinical markers of success and understanding how blood flow can affect cell migration is of upmost importance.[15] In contrast to the work by[14] where cells tended to migrate in the direction of the steady flow field, the POD results herein show that endothelial cells under pulsatile fluid flow tend to migrate against the net flow direction. This difference highlights the possibility that migrating endothelial cells react to steady and pulsatile flow differently.[22]

Another advantage of the POD order reduction method is that the amplitude of the mode coefficients is proportional to the trajectory of the cells, so that the influence of each POD trajectory mode can be ascertained by close observation of the value of the mode amplitude coefficient per Eq. (5) (Fig. 3b). Figure 2c clearly shows that the cell displacement described by mode 1 was more representative of cell trajectories closer to the edge of the wound than cells further away, which is a type of analysis often inaccessible with other methods, such as cell front models.[18,21] In contrast, single cell models capture the temporal displacement of cells, while missing the intercellular influence that can affect migration.[9] The POD method easily adapted to changes in migratory patterns due to the different fluid flow waveforms resulting in the changes of the shape and amplitude of the POD trajectory modes and coefficients, respectively, while models such as the Fisher equation can adequately describe cell migration in some instances, but fail in others.[30]

A major distinction between different models of cell migration, such as the phase-field, polygonal, cellular Potts, and spherical cells is that these models represent biochemical and biophysical reactions mathematically and the accuracy of the results strongly depends on the assumptions made, and they tend to be more computationally expensive.[4] In contrast, POD does not model biophysical interactions and biochemical reactions, but

extracts information from the cell motions. Since the POD modes are dependent on the information extracted from the cell motions, the POD trajectory mode shapes will change when the cell motions change due to different stimuli as observed herein with respect to different fluid flow waveforms. The dependence of the POD method on experimental data is a major distinction from mathematical models, yet sufficient data from POD analyses could be used to construct artificial intelligence models based on cell migration data from experiments.

In the results discussed here, the centroid of endothelial cell nuclei, instead of the cell centroid, were tracked. Given that endothelial cells tend to display either a cobblestone or spindle-like symmetric shape, it was assumed that cell centroid coincided with the nucleus centroid. Instances where the nucleus center did not coincide with the cell centroid may affect the accuracy of the tracked location.

Although the experiments herein assessed cell migration under different fluid flow conditions using a two-dimensional wound healing assay, this approach is certainly amenable for simplification of three dimensional cell migration trajectories to lower order data sets. The potential for using POD order reduction methods to develop artificial intelligence approaches to model cell migration under different stimuli is invaluable. Analogous to the significant role that computational fluid dynamics and finite element methods have contributed in the solving of equations that are derived based on first principles, POD-based analyses have the potential of playing a similar role in dealing with analysis of big data that are collected experimentally. POD-based artificial intelligence models could serve a role in *in silico* testing of different therapeutic treatments and strategies.

ACKNOWLEDGMENTS

We thank Dr. Melissa D. Sánchez for constructive feedback and criticism. This work was supported by NSF grants CAREER CMMI 1842308 (to J.M.J.) and CBET 1605060 (to Y.M.).

CONFLICT OF INTEREST

The authors have no conflicts of interest to disclose.

REFERENCES

[1]Albuquerque, M. L. C., C. M. Waters, U. Savla, H. W. Schnaper, and A. S. Flozak. Shear stress enhances human endothelial cell wound closure in vitro. *Am. J. Physiol. Heart Circ. Physiol.* 279:H293–H302, 2000.

[2]Alert, R. and X. Trepat. Physical models of collective cell migration. *Annu. Rev. Condens. Matter Phys.* 11:77–101, 2020.

[3]Ando, J., H. Nomura, and A. Kamiya. The effect of fluid shear stress on the migration and proliferation of cultured endothelial cells. *Microvasc. Res.* 33:62–70, 1987.

[4]Buttenschön, A. and L. Edelstein-Keshet. Bridging from single to collective cell migration: a review of models and links to experiments. *PLoS Comput. Biol.* 16:e1008411, 2020.

[5]Camley, B. A. and W.-J. Rappel. Physical models of collective cell motility: from cell to tissue. *J. Phys. D Appl. Phys.* 50:113002, 2017.

[6]Codling, E. A., M. J. Plank, and S. Benhamou. Random walk models in biology. *J. R. Soc. Interface* 5:813–834, 2008.

[7]Danuser, G., J. Allard, and A. Mogilner. Mathematical modeling of eukaryotic cell migration: insights beyond experiments. *Annu. Rev. Cell Dev. Biol.* 29:501–528, 2013.

[8]DePaola, N., M. A. Gimbrone Jr, P. F. Davies, and C. F. Dewey Jr. Vascular endothelium responds to fluid shear stress gradients. *Arterioscler. Thromb. J. Vasc. Biol.* 12:1254–1257, 1992.

[9]Dieterich, P., R. Klages, R. Preuss, and A. Schwab. Anomalous dynamics of cell migration. *Proc. Natl. Acad. Sci.* 105:459–463, 2008.

[10]Discher, D. E., P. Janmey, and Y.-L. Wang. Tissue cells feel and respond to the stiffness of their substrate. *Science* 310:1139–1143, 2005.

[11]Doran, M. R., R. J. Mills, A. J. Parker, K. A. Landman, and J. J. Cooper-White. A cell migration device that maintains a defined surface with no cellular damage during wound edge generation. *Lab Chip* 9:2364–2369, 2009.

[12]Franco, D., F. Milde, M. Klingauf, F. Orsenigo, E. Dejana, D. Poulikakos, M. Cecchini, P. Koumoutsakos, A. Ferrari, and V. Kurtcuoglu. Accelerated endothelial wound healing on microstructured substrates under flow. *Biomaterials* 34:1488–1497, 2013.

[13]Habbal, A., H. Barelli, and G. Malandain. Assessing the ability of the 2d fisher-kpp equation to model cell-sheet wound closure. *Math. Biosci.* 252:45–59, 2014.

[14]Hsu, P.-P., S. Li, Y.-S. Li, S. Usami, A. Ratcliffe, X. Wang, and S. Chien. Effects of flow patterns on endothelial cell migration into a zone of mechanical denudation. *Biochem. Biophys. Res. Commun.* 285:751–759, 2001.

[15]Inoue, T., K. Croce, T. Morooka, M. Sakuma, K. Node, D. I. Simon. Vascular inflammation and repair: implications for re-endothelialization, restenosis, and stent thrombosis. *JACC Cardiovasc. Interv.* 4:1057–1066, 2011.

[16]Jiang, Y.-Z., J. M. Jiménez, K. Ou, M. E. McCormick, L.-D. Zhang, and P. F. Davies. Hemodynamic disturbed flow induces differential dna methylation of endothelial kruppel-like factor 4 promoter in vitro and in vivo. *Circ. Res.* 115:32–43, 2014.

[17]Jiménez, J. M., V. Prasad, M. D. Yu, C. P. Kampmeyer, A.-H. Kaakour, P.-J. Wang, S. F. Maloney, N. Wright, I. Johnston, Y.-Z. Jiang, and P. F. Davies. Macro-and microscale variables regulate stent haemodynamics, fibrin

deposition and thrombomodulin expression. *J. R. Soc. Interface* 11:20131079, 2014.
[18]Johnston, S. T., M. J. Simpson, and D. S. McElwain. How much information can be obtained from tracking the position of the leading edge in a scratch assay? *J. R. Soc. Interface* 11:20140325, 2014.
[19]Ladoux, B. and R.-M. Mège. Mechanobiology of collective cell behaviours. *Nat. Rev. Mol. Cell Biol.* 18:743–757, 2017.
[20]Maini, P. K., D. S. McElwain, and D. Leavesley. Travelling waves in a wound healing assay. *Appl. Math. Lett.* 17:575–580, 2004.
[21]Maini, P. K., D. S. McElwain, and D. I. Leavesley. Traveling wave model to interpret a wound-healing cell migration assay for human peritoneal mesothelial cells. *Tissue Eng.* 10:475–482, 2004.
[22]Nguyen, D. T., A. F. Smith, and J. M. Jiménez. Stent strut streamlining and thickness reduction promote endothelialization. *J. R. Soc. Interface* 18:20210023, 2021.
[23]Nikolic, D. L., A. N. Boettiger, D. Bar-Sagi, J. D. Carbeck, and S. Y. Shvartsman. Role of boundary conditions in an experimental model of epithelial wound healing. *Am. J. Physiol. Cell Physiol.* 291:C68–C75, 2006.
[24]Osborne, J. M., A. G. Fletcher, J. M. Pitt-Francis, P. K. Maini, and D. J. Gavaghan. Comparing individual-based approaches to modelling the self-organization of multicellular tissues. *PLoS Comput. Biol.* 13:e1005387, 2017.
[25]Pinnau, R. Model reduction via proper orthogonal decomposition. In Model Order Reduction: Theory Research Aspects and Applications, edited by W. H. A. Schilders, H A. van der Vorst, and J. Rommes. Berlin: Springer, 2008, pp. 95–109.
[26]Poujade, M., E. Grasland-Mongrain, A. Hertzog, J. Jouanneau, P. Chavrier, B. Ladoux, A. Buguin, and P. Silberzan. Collective migration of an epithelial monolayer in response to a model wound. *Proc. Nati. Acad. Sci.* 104:15988–15993, 2007.
[27]Rathinam, M. and L. R. Petzold. Dynamic iteration using reduced order models: a method for simulation of large scale modular systems. *SIAM J. Numer. Anal.* 40:1446–1474, 2002.
[28]Rathinam, M. and L. R. Petzold. A new look at proper orthogonal decomposition. *SIAM J. Numer. Anal.* 41:1893–1925, 2003.
[29]Savla, U., L. E. Olson, and C. M. Waters. Mathematical modeling of airway epithelial wound closure during cyclic mechanical strain. *J. Appl. Physiol.* 96:566–574, 2004.
[30]Sengers, B. G., C. P. Please, and R. O. Oreffo. Experimental characterization and computational modelling of two-dimensional cell spreading for skeletal regeneration. *J. R. Soc. Interface* 4:1107–1117, 2007.
[31]Smith, J. T., J. T. Elkin, and W. M. Reichert. Directed cell migration on fibronectin gradients: effect of gradient slope. *Exp. Cell Res.* 312:2424–2432, 2006.
[32]Stefopoulos, G., F. Robotti, V. Falk, D. Poulikakos, and A. Ferrari. Endothelialization of rationally microtextured surfaces with minimal cell seeding under flow. *Small* 12:4113–4126, 2016.
[33]Sweet, D. T., J. M. Jiménez, J. Chang, P. R. Hess, P. Mericko-Ishizuka, J. Fu, L. Xia, P. F. Davies, M. L. Kahn et al. Lymph flow regulates collecting lymphatic vessel maturation in vivo. *J. Clin. Investig.* 125:2995–3007, 2015.
[34]Takamizawa, K., S. Niu, and T. Matsuda. Mathematical simulation of unidirectional tissue formation: in vitro transanastomotic endothelialization model. *J. Biomater. Sci. Polym. Ed.* 8:323–334, 1997.
[35]Yamamoto, T., Y. Ogasawara, A. Kimura, H. Tanaka, O. Hiramatsu, K. Tsujioka, M. J. Lever, K. H. Parker, C. J. Jones, C. G. Caro et al. Blood velocity profiles in the human renal artery by doppler ultrasound and their relationship to atherosclerosis. *Arterioscler. Thromb. Vasc. Biol.* 16:172–177, 1996.
[36]Zhao, M. Electrical fields in wound healing-an overriding signal that directs cell migration. Regenerative biology and medicine: II and patterning and evolving the vertebrate forebrain. *Semin. Cell Dev. Biol.* 20:674–682, 2009.